RadioGraphics

State-of-the-Art Imaging of Acute Stroke[1]

Ashok Srinivasan, MD • Mayank Goyal, MD • Faisal Al Azri, MD
Cheemun Lum, MD

CME FEATURE

See accompanying test at http://www.rsna.org/education/rg_cme.html

LEARNING OBJECTIVES FOR TEST 4

After reading this article and taking the test, the reader will be able to:

- Describe the basic principles of CT and MR techniques used to evaluate acute stroke, including conventional, angiographic, and diffusion and perfusion imaging techniques.
- Determine an appropriate imaging protocol for acute stroke evaluation.
- Recognize the significance of a penumbra for therapy planning and prognosis after acute stroke.

TEACHING POINTS

See last page

Stroke is a leading cause of mortality and morbidity in the developed world. The goals of an imaging evaluation for acute stroke are to establish a diagnosis as early as possible and to obtain accurate information about the intracranial vasculature and brain perfusion for guidance in selecting the appropriate therapy. A comprehensive evaluation may be performed with a combination of computed tomography (CT) or magnetic resonance (MR) imaging techniques. Unenhanced CT can be performed quickly, can help identify early signs of stroke, and can help rule out hemorrhage. CT angiography and CT perfusion imaging, respectively, can depict intravascular thrombi and salvageable tissue indicated by a penumbra. These examinations are easy to perform on most helical CT scanners and are increasingly used in stroke imaging protocols to decide whether intervention is necessary. While acute infarcts may be seen early on conventional MR images, diffusion-weighted MR imaging is more sensitive for detection of hyperacute ischemia. Gradient-echo MR sequences can be helpful for detecting a hemorrhage. The status of neck and intracranial vessels can be evaluated with MR angiography, and a mismatch between findings on diffusion and perfusion MR images may be used to predict the presence of a penumbra. The information obtained by combining various imaging techniques may help differentiate patients who do not need intravenous or intraarterial therapy from those who do, and may alter clinical outcomes.

Abbreviations: ADC = apparent diffusion coefficient, ASPECTS = Alberta Stroke Program Early CT Score, MCA = middle cerebral artery, NIHSS = National Institutes of Health Stroke Score, ROI = region of interest

RadioGraphics 2006; 26:S75–S95 • **Published online** 10.1148/rg.26si065501 • **Content Codes:** CT MR NR

[1]From the Department of Diagnostic Imaging, University of Ottawa, Ottawa Hospital, Ottawa, Ontario, Canada. Recipient of a Certificate of Merit award for an education exhibit at the 2005 RSNA Annual Meeting. Received January 13, 2006; revision requested May 9 and received June 13; accepted June 28. All authors have no financial relationships to disclose. **Address correspondence to** A.S., Department of Radiology, Division of Neuroradiology, University of Michigan Health System, 1500 E Medical Center Dr, Ann Arbor, MI 48109 (e-mail: *ashoks@med.umich.edu*).

Introduction

Stroke can be defined as an acute central nervous system injury with an abrupt onset. Acute ischemia constitutes approximately 80% of all strokes and is an important cause of morbidity and mortality in the United States (1). Before effective therapies were introduced for acute ischemic stroke, imaging was used primarily to exclude hemorrhage and other mimics of stroke, such as infection and neoplasm. The development of new treatment options in any clinical scenario constantly necessitates the further evolution of imaging technology. In acute stroke, impetus was provided by findings in the National Institute for Neurological Diseases and Stroke trial, in which a clinical benefit was demonstrated for intravenous thrombolytic drug therapy in cases of acute stroke (2). Investigators in subsequent trials showed good clinical outcomes of thrombolytic drug therapy in patients with acute stroke who were selected on the basis of imaging criteria (3). The concept of salvageable brain tissue (indicated by a penumbra on brain images) has driven the development of functional imaging techniques such as brain perfusion imaging.

Imaging in patients with acute stroke should be targeted toward assessment of the four *P*s—parenchyma, pipes, perfusion, and penumbra—as described by Rowley (4) and summarized in Table 1. This approach enables the detection of intracranial hemorrhage, differentiation of infarcted tissue from salvageable tissue, identification of intravascular thrombi, selection of the appropriate therapy, and prediction of the clinical outcome.

In this article, we explain the significance of a penumbra and discuss the underlying principles and clinical applications of state-of-the-art computed tomography (CT) and magnetic resonance (MR) imaging techniques in acute stroke evaluation. We also briefly compare the utility of CT and MR imaging for acute stroke evaluation and describe the acute stroke imaging protocol used at our institution.

Significance of a Penumbra

Unlike muscle, brain tissue is exquisitely sensitive to ischemia, because of the absence of neuronal energy stores. In the complete absence of blood flow, the available energy can maintain neuronal viability for approximately 2–3 minutes. However, in acute stroke, ischemia is more often incomplete, with the injured area of the brain receiving a collateral blood supply from uninjured arterial and leptomeningeal territories. Therefore,

Table 1
Goals of Acute Stroke Imaging

Parenchyma	Assess early signs of acute stroke, rule out hemorrhage
Pipes	Assess extracranial circulation (carotid and vertebral arteries of the neck) and intracranial circulation for evidence of intravascular thrombus
Perfusion	Assess cerebral blood volume, cerebral blood flow, and mean transit time
Penumbra	Assess tissue at risk of dying if ischemia continues without recanalization of intravascular thrombus

Source.—Reference 4.

Teaching Point

acute cerebral ischemia may result in a central irreversibly infarcted tissue core surrounded by a peripheral region of stunned cells that is called a penumbra (Fig 1a). Evoked potentials in the peripheral region are abnormal, and the cells have ceased to function, but this region is potentially salvageable with early recanalization (5,6).

The sequence of events initiated by a decrease in cerebral perfusion is depicted in Figure 1b. There is an initial cessation of neuronal protein synthesis, followed by a loss of membrane transport and synaptic activity. Further reduction in perfusion pressure eventually causes irreversible infarction. The transition from ischemia to irreversible infarction depends on both the severity and the duration of the diminution of blood flow. Other factors that influence this transition include the selective vulnerability of specific neuronal populations and physiologic conditions during recanalization (5,6). The penumbra is a dynamic entity that exists within a narrow range of perfusion pressures, and the duration of the delay in recanalization is inversely related to the size of the penumbra (5).

A penumbra can be evaluated both on CT images (on which it is evidenced by a discrepancy in perfusion parameters) and on MR images (on which it is indicated by a mismatch between diffusion and perfusion parameters). The presence of a penumbra has important implications for selection of the appropriate therapy and prediction of the clinical outcome. Intravenous thrombolytic treatment is not typically administered to patients with acute stroke beyond the conventional 3-hour period after the onset of symptoms, because such treatment results in an increased risk of hemorrhage (2). However, the results of recent studies have demonstrated that intravenous thrombolytic therapy may benefit patients who are carefully selected according to findings of a diffusion or perfusion mismatch or a penumbra at imaging (3,7).

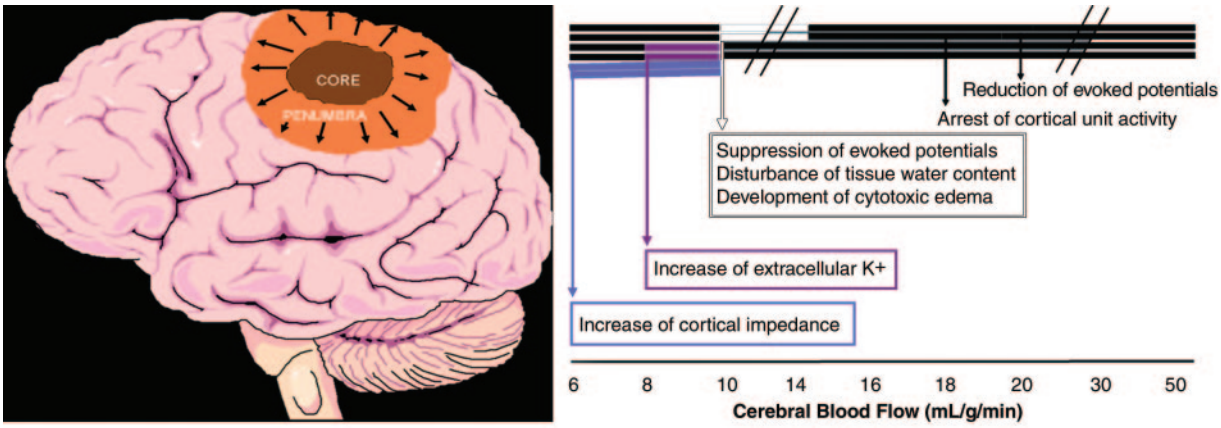

Figure 1. **(a)** Schematic of brain involvement in acute stroke shows a core of irreversibly infarcted tissue surrounded by a peripheral region of ischemic but salvageable tissue referred to as a penumbra. Without early recanalization, the infarction gradually expands to include the penumbra. **(b)** Diagram shows the evolution of events at a microscopic level with decreasing cerebral perfusion (from right to left). Irreversible cell death generally occurs when cerebral blood flow decreases to less than 10 mL/100 g/min.

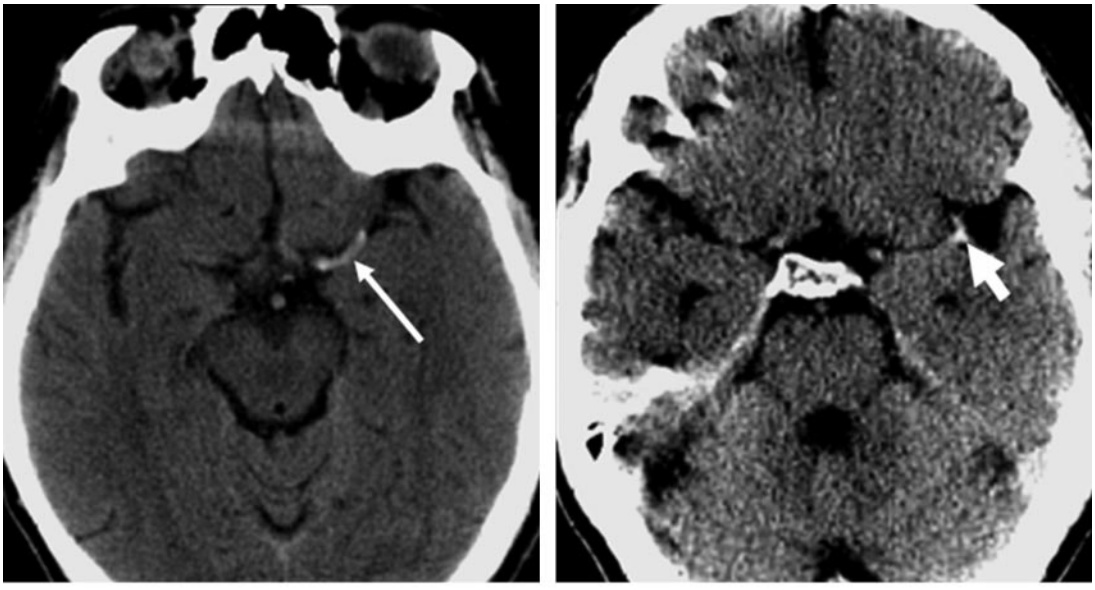

Figure 2. Axial unenhanced CT images in a proximal segment of the left MCA in a 53-year-old man **(a)** and a distal segment of the left MCA in a 62-year-old woman **(b)**, obtained 2 hours after the onset of right hemiparesis and aphasia, show areas of hyperattenuation (arrow) suggestive of intravascular thrombi.

Role of CT in Acute Stroke Evaluation

In this section, the role of state-of-the-art CT in acute stroke evaluation is highlighted. The three key CT techniques—unenhanced imaging, angiography, and perfusion imaging—are discussed individually but may be used in combination.

Unenhanced CT

Unenhanced CT is widely available, can be performed quickly, and does not involve the administration of intravenous contrast material. It not only can help identify a hemorrhage (a contraindication to thrombolytic therapy), but it also can help detect early-stage acute ischemia by depicting features such as the hyperdense vessel sign, the insular ribbon sign, and obscuration of the lentiform nucleus. The last two features are caused by a loss of contrast between gray matter and white matter on CT images (8).

An acute thrombus in an intracranial vessel typically has high attenuation. This feature is referred to as the hyperdense vessel sign (or, in cases of middle cerebral artery [MCA] involvement, hyperdense MCA sign) (Fig 2). Although

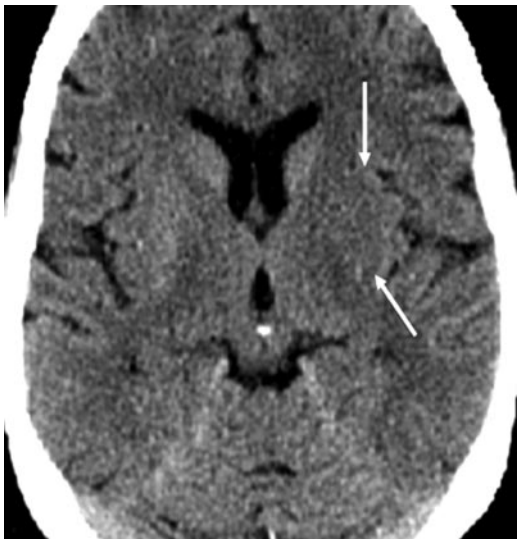

Figure 3. Axial unenhanced CT image obtained in a 53-year-old man (same patient as in Fig 2a) shows hypoattenuation and obscuration of the left lentiform nucleus (arrows), which, because of acute ischemia in the lenticulostriate distribution, appears abnormal in comparison with the right lentiform nucleus.

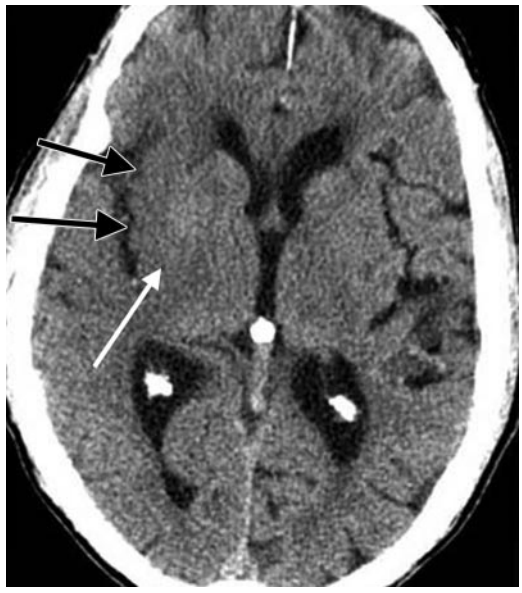

Figure 4. Axial unenhanced CT image, obtained in a 73-year-old woman 2½ hours after the onset of left hemiparesis, shows hypoattenuation and obscuration of the posterior part of the right lentiform nucleus (white arrow) and a loss of gray matter–white matter definition in the lateral margins of the right insula (black arrows). The latter feature is known as the insular ribbon sign.

this sign is highly specific, its sensitivity is poor (9). A hyperdense MCA sign also may be seen in the presence of a high hematocrit level or MCA calcification, but in such cases the hyperattenuation is usually bilateral (10–13). Rarely, fat emboli appear hypoattenuated when compared with attenuation in the contralateral vessel (14).

Acute ischemia of the lenticulostriate territory may result in obscuration of the lentiform nucleus, which appears hypoattenuated because of cytotoxic edema (Fig 3). This feature may be seen on CT images within 2 hours after the onset of a stroke (15).

Cytotoxic edema of the insular cortex, which is susceptible to early and irreversible ischemic damage, also causes local hypoattenuation, which results in the so-called insular ribbon sign (Fig 4) (16).

Importance of Window Settings.—Lev et al (17) showed sensitivity and specificity of 57% and 100%, respectively, for acute ischemic stroke detection at unenhanced CT with the use of standard window settings (width, 80 HU; center, 20 HU). Sensitivity increased to 71% with a change of window width and center level settings to 8 HU and 32 HU, respectively, without a loss in specificity. Hence, detection of early acute ischemic stroke on unenhanced CT images may be improved by using variable window width and center level settings to accentuate the contrast between normal and edematous tissue (Fig 5).

Teaching Point

Quantitation of Ischemic Involvement.—In the European Cooperative Acute Stroke Study trial, involvement of more than one-third of the MCA territory depicted at unenhanced CT was a criterion for the exclusion of patients from thrombolytic therapy because of a potential increase in the risk for hemorrhage (18). However, the results of subsequent studies with use of the one-third rule showed poor interobserver correlation, primarily because of variability in the level of axial CT images (19–22).

The Alberta Stroke Program Early CT Score (ASPECTS) was proposed in 2001 as a means of quantitatively assessing acute ischemia on CT images by using a 10-point topographic scoring

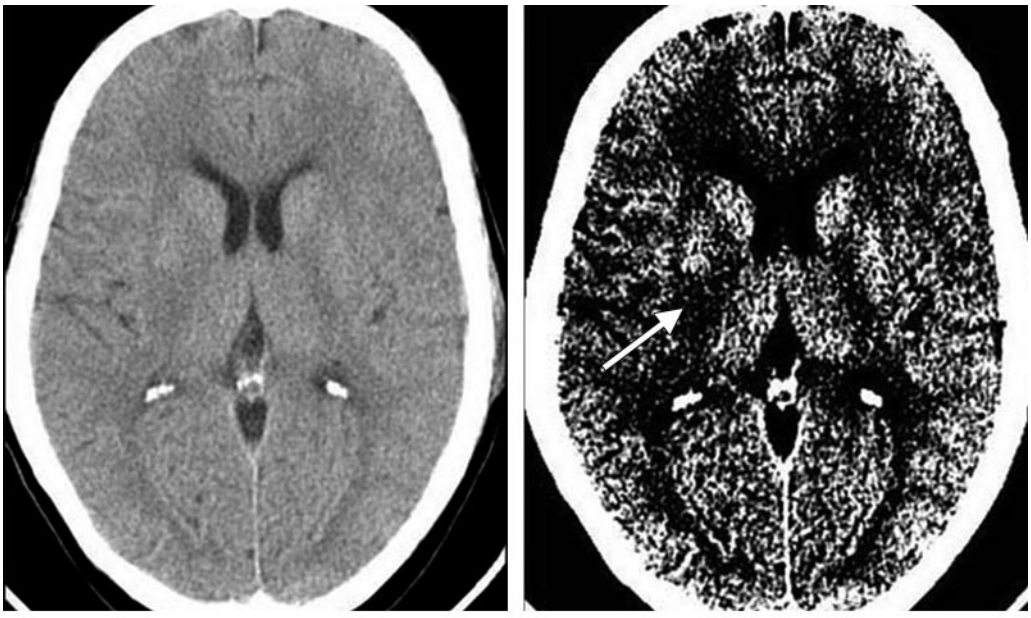

a. b.

Figure 5. Axial unenhanced CT images, obtained in a 45-year-old man 2 hours after the onset of left hemiparesis, show obscuration of the right lentiform nucleus (arrow in **b**). This feature is less visible with the routine brain imaging window used for **a** (window width, 80 HU; center, 35 HU) than with the narrower window used for **b** (window width, 10 HU; center, 28 HU).

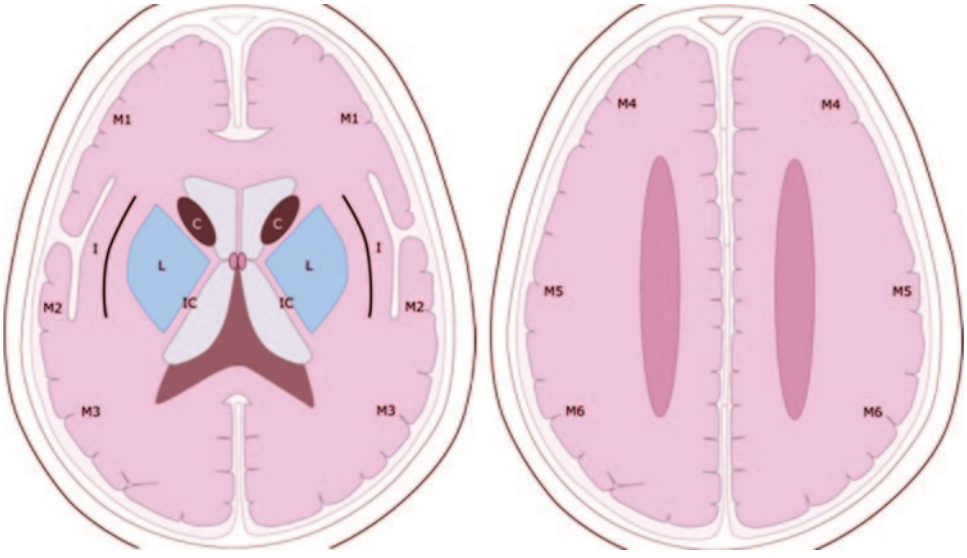

Figure 6. Schematic shows the 10 regions of the MCA distribution, each of which accounts for one point in the ASPECTS system: M1, M2, M3, M4, M5, M6, the caudate nucleus *(C)*, the lentiform nucleus *(L)*, the internal capsule *(IC)*, and the insular cortex *(I)*. For each area involved in ischemia depicted at unenhanced CT, one point is subtracted from the total score of 10.

system (23). According to this system, the MCA territory is divided into 10 regions, each of which accounts for one point in the total score (Fig 6). The normal MCA territory is assigned a total score of 10. For each area involved in stroke on the unenhanced CT images, one point is deducted from that score. Hence, a score of 0

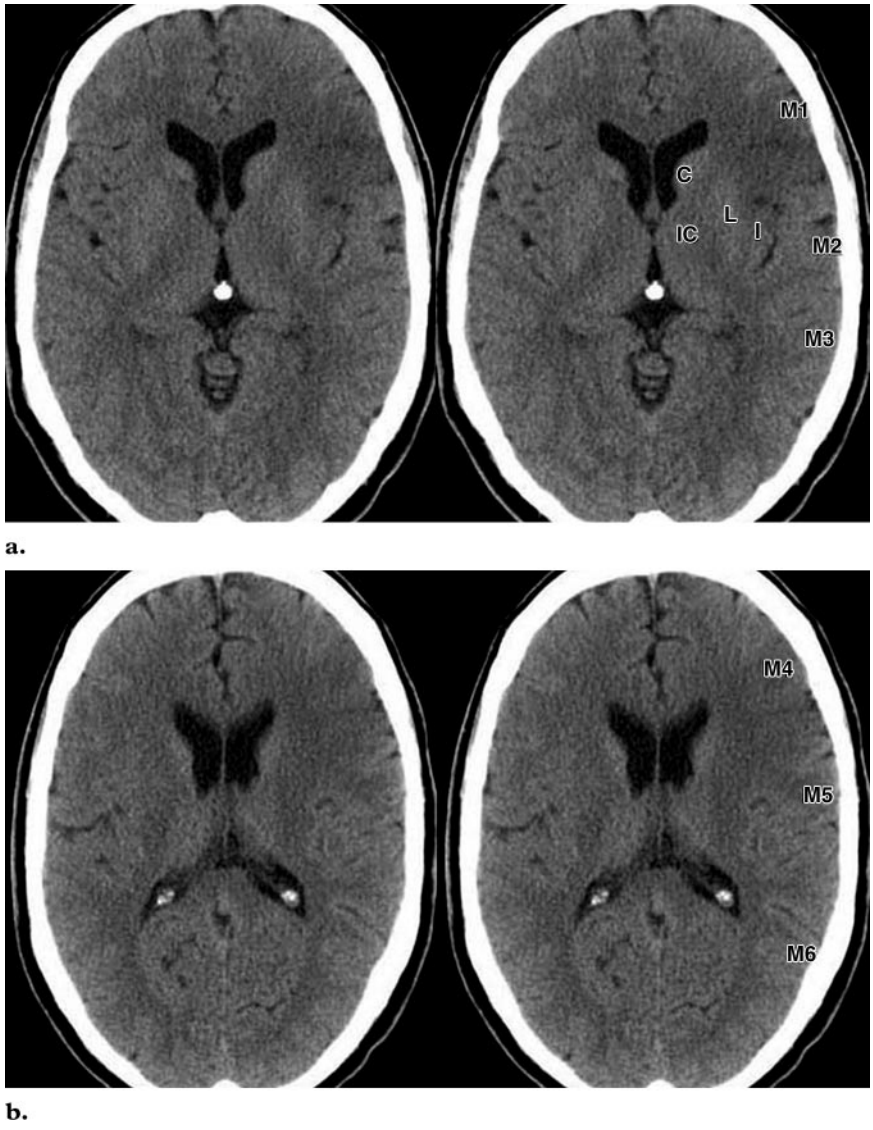

Figure 7. Unenhanced CT images in a 56-year-old man with right hemiparesis (**a** at a lower level than **b**) demonstrate involvement of the M1 region, insular cortex *(I)*, and lentiform nucleus *(L)*. Thus, three points are subtracted from the 10-point ASPECTS, and the final score is seven points. *C* = caudate nucleus, *IC* = internal capsule.

translates into a finding of diffuse ischemic involvement throughout the MCA territory (Fig 7). It was demonstrated that the baseline ASPECTS correlated inversely with the National Institutes of Health Stroke Score (NIHSS), and, as the ASPECTS decreased, the probability of dependence, death, and symptomatic hemorrhage increased. In addition, clinical agreement with the ASPECTS was superior to that with the one-third MCA rule. The authors concluded that the ASPECTS system is a systematic, robust, and practical method that is applicable to axial images acquired at different levels (23).

Thus, unenhanced CT plays an important role in the identification and quantification of parenchymal involvement in acute stroke.

Table 2
CT Angiography Protocol with a 16-Section Multidetector CT Scanner

Coverage	Aortic arch to circle of Willis
Scanning parameters	120 kV, 260 mAs
Scanning delay	Dependent on ROI placed over aortic arch to detect contrast medium bolus (or empiric delay of 25 sec)
Contrast medium dose	100–120 mL of a nonionic contrast medium (300 mg of iodine per milliliter) at the rate of 3–4 mL/sec
Section thickness	2.5 mm
Section reconstruction	1.25 mm

CT Angiography

CT angiography is a widely available technique for assessment of both the intracranial and extracranial circulation. Its utility in acute stroke lies in its capabilities for demonstrating thrombi within intracranial vessels and for evaluating the carotid and vertebral arteries in the neck (24).

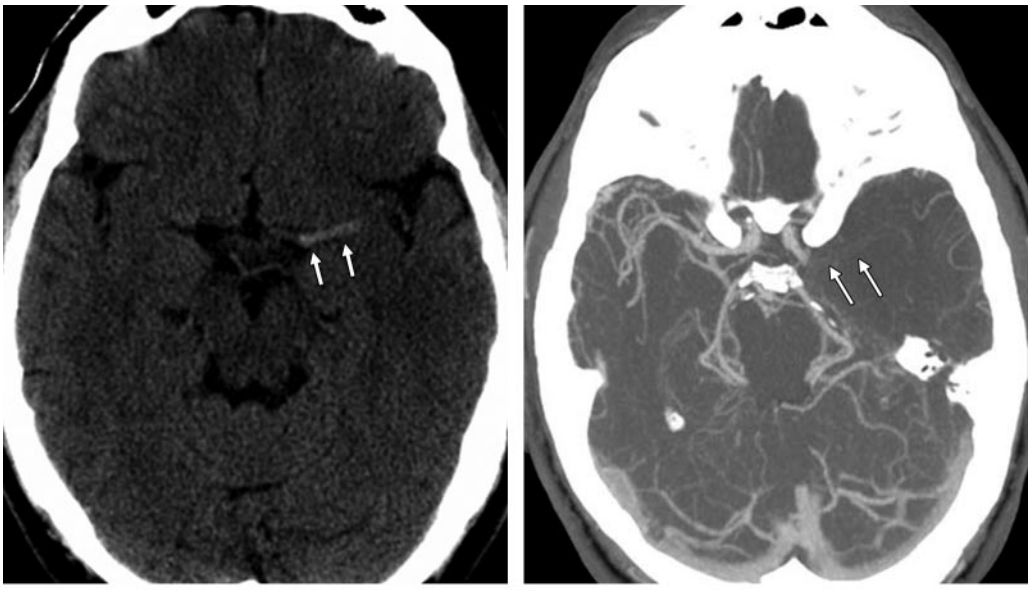

a. b.

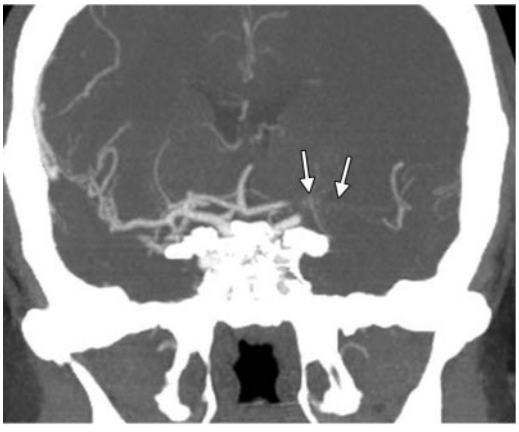

c.

Figure 8. **(a)** Unenhanced CT image in a 72-year-old woman with acute right hemiplegia shows hyperattenuation in a proximal segment of the left MCA (arrows). **(b, c)** Axial **(b)** and coronal **(c)** reformatted images from CT angiography show the apparent absence of the same vessel segment (arrows). The presence of an intravascular thrombus in this location was confirmed by comparing the reformatted images with the CT source images (not shown).

CT angiography typically involves a volumetric helical acquisition that extends from the aortic arch to the circle of Willis. The examination is performed by using a time-optimized bolus of contrast material for vessel enhancement (24). The CT angiography protocol used at our institution is summarized in Table 2. Postprocessing is performed at a three-dimensional display workstation to generate multiplanar reformatted images and maximum intensity projection images.

Intraarterial thrombolysis may be more efficacious than intravenous therapy in patients with acute stroke and a significant thrombus burden (25,26). Therefore, the CT angiographic demonstration of a significant thrombus burden can guide appropriate therapy in the form of intraarterial or mechanical thrombolysis. Furthermore, the identification of carotid artery disease and visualization of the aortic arch may provide clues to the cause of the ischemic event and guidance for the interventional neuroradiologist (Fig 8).

Correlation between the location of intravascular occlusions on CT angiograms and clinical outcome parameters such as the initial NIHSS also has been demonstrated for multiple occlusions in the M1 and M2 regions and absent occlusions (27). In this study, patients with patent intracranial vessels or with one or more occult distal occlusions on CT angiograms before thrombolytic treatment had a lower NIHSS and a better chance of early improvement and early independence, with fewer hemorrhages.

Thus, CT angiography is useful for evaluating the intracranial and extracranial vessels and guiding appropriate therapy.

CT Perfusion Imaging

CT perfusion imaging can be used to measure the following perfusion parameters: cerebral blood volume (ie, the volume of blood per unit of brain tissue; normal range, 4–5 mL/100 g); cerebral blood flow (ie, the volume of blood flow per unit of brain tissue per minute; normal range in gray matter, 50–60 mL/100 g/min); mean transit time, defined as the time difference between the arterial inflow and venous outflow; and time to peak enhancement, which represents the time from the beginning of contrast material injection

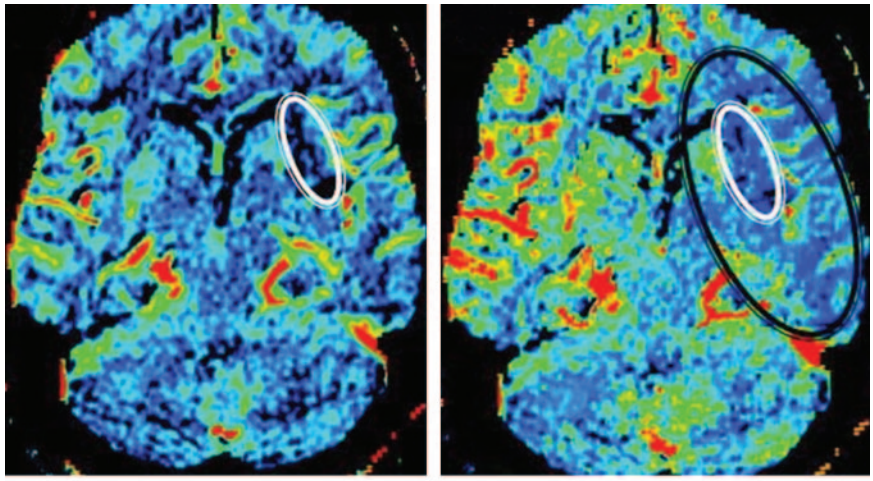

Figure 9. CT perfusion maps of cerebral blood volume **(a)** and cerebral blood flow **(b)** show, in the left hemisphere, a region of decreased blood volume (white oval) that corresponds to the ischemic core and a larger region of decreased blood flow (black oval in **b**) that includes the ischemic core and a peripheral region of salvageable tissue. The difference between the two maps (black oval − white oval) is the penumbra.

Table 3
CT Perfusion Imaging Protocol with a 16-Section Multidetector CT Scanner

Coverage	Four sections chosen by the radiologist from the unenhanced CT images
Scanning parameters	80 kV, 105 mAs
Section thickness	5 mm
Scanning delay	5 sec
Scanning duration	45 sec
Contrast medium dose	50 mL of a nonionic contrast medium (300 mg of iodine per milliliter) at the rate of 4–5 mL/sec

Table 4
Steps in CT Perfusion Data Postprocessing

Freehand or automated placement of an ROI over an input artery to obtain the arterial time-attenuation curve or arterial input function
Freehand or automated placement of an ROI over an input vein to obtain the venous time-attenuation curve
Generation of the arterial and venous time-attenuation curves
Deconvolution analysis of arterial and tissue time-attenuation curves to obtain the mean transit time
Calculation of cerebral blood volume from the area under the curve in a parenchymal pixel divided by the area under the curve in an arterial pixel
Calculation of cerebral blood flow by using the central volume principle (CBF = CBV/MTT)

Note.—CBF = cerebral blood flow, CBV = cerebral blood volume, MTT = mean transit time.

to the maximum concentration of contrast material within a region of interest (ROI) (8).

Compared with MR imaging, xenon-enhanced CT, positron emission tomography, and single photon emission CT, CT perfusion imaging is more widely available and can be performed quickly on any standard helical CT scanner immediately after unenhanced CT. CT perfusion maps then can be generated in a short time at an appropriate workstation (28). CT perfusion imaging also allows quantitative and qualitative evaluation of the cerebral blood volume, cerebral blood flow, and mean transit time. The clinical application of CT perfusion imaging in acute stroke is based on the hypothesis that the penumbra shows either *(a)* increased mean transit time with moderately decreased cerebral blood flow (>60%) and normal or increased cerebral blood volume (80%–100% or higher) secondary to autoregulatory mechanisms or *(b)* increased mean transit time with markedly reduced cerebral blood flow (>30%) and moderately reduced cerebral blood volume (>60%), whereas infarcted tissue shows severely decreased cerebral blood flow (<30%) and cerebral blood volume (<40%) with increased mean transit time (Fig 9) (29,30).

Teaching Point

The evaluation of brain perfusion is based on the central volume principle, according to which CBF = CBV/MTT, where CBF is the cerebral blood flow, CBV is the cerebral blood volume, and MTT is the mean transit time. The evaluation of perfusion imaging data requires the use of complex deconvolution algorithms to produce perfusion maps (30,31). The two most commonly used CT perfusion imaging techniques are dynamic contrast material–enhanced perfusion imaging and perfused-blood-volume mapping.

Dynamic Contrast-enhanced CT.—Based on the multicompartmental tracer kinetic model, dynamic CT perfusion imaging is performed by monitoring the first pass of an iodinated contrast agent bolus through the cerebral circulation. The

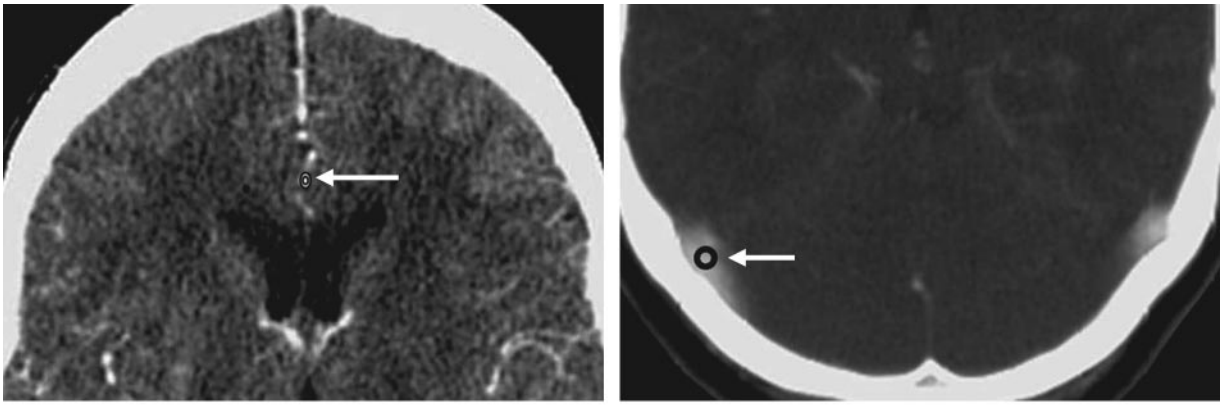

a. b.

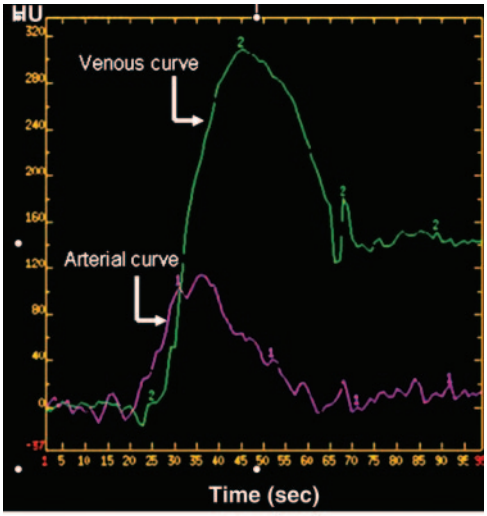

c.

Figure 10. The steps involved in the postprocessing of CT perfusion data include the placement of ROIs in an arterial pixel (arrow in **a**) and a venous pixel (arrow in **b**) and the generation of a time-attenuation curve **(c)** for each ROI. The curves are then used to formulate color-coded CT perfusion maps.

contrast agent bolus causes a transient increase in attenuation that is linearly proportional to the amount of contrast material in a given region. This principle is used to generate time-attenuation curves for an arterial ROI, a venous ROI, and each pixel. The perfusion parameters then can be calculated by employing mathematical modeling techniques such as deconvolution analysis (29,30).

Dynamic CT perfusion imaging typically is performed on a helical CT scanner after the acquisition of unenhanced CT images. Depending on the CT detector configuration, two to four sections, each with a thickness of 5, 6, 8, 10, or 12 mm, may be obtained. The imaging volume is chosen on the basis of the unenhanced CT images, and, typically, at least one of the axial sections passes through the level of the basal ganglia, because this level contains representative territories supplied by the anterior, middle, and posterior cerebral arteries (32). Dynamic CT perfusion imaging at our institution is performed by using a 16-section multidetector CT scanner (LightSpeed; GE Medical Systems, Milwaukee, Wis). The details of the imaging protocol are listed in Table 3.

Deconvolution analysis is probably the most commonly used algorithm for dynamic CT perfusion data postprocessing because of its advantages over other methods, namely the absence of unrealistic assumptions about venous outflow and the ability to use lower intravenous infusion rates. With this method, the regional mean transit time is calculated by performing a deconvolution of the regional (tissue) time-attenuation curve with respect to the arterial time-attenuation curve (arterial input function). The cerebral blood volume is calculated by dividing the area under the time-attenuation curve in a parenchymal pixel by the area under the time-attenuation curve in an arterial pixel. The central volume equation then can be solved to obtain the cerebral blood flow (29,30). In addition, visual assessment of the venous time-attenuation curve is important for the normalization of perfusion parameters because it helps correct the data for partial volume averaging effects (32).

Both the arterial and the venous ROIs are optimally chosen in large vessels that course in a direction nearly perpendicular to the plane of CT acquisition (the axial plane). The arterial ROI is typically chosen in either of the two anterior cerebral arteries (if they are unaffected) or in the unaffected MCA. The venous ROI is usually placed over the superior sagittal sinus, transverse sinus, or torcular herophili. Color-coded perfusion maps of cerebral blood volume, cerebral blood flow, and mean transit time are then generated at the workstation (30,33). At our institution, we analyze our CT perfusion source image data at an off-line imaging workstation (Advantage Windows). The steps involved in postprocessing are described in a simplified form in Table 4, and the placement of ROIs is shown in Figure 10.

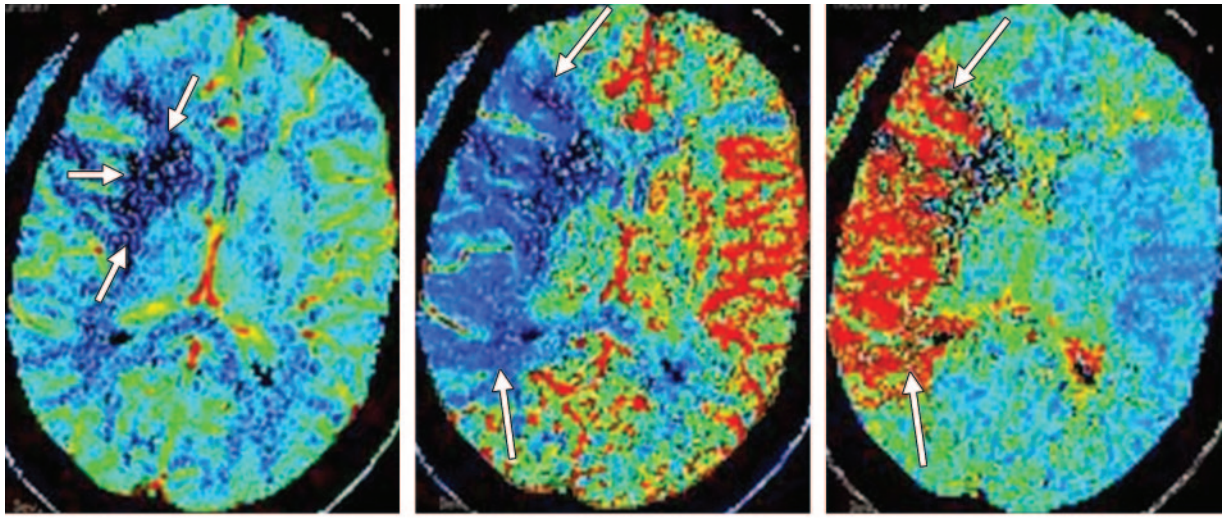

a. b. c.

Figure 11. Acute stroke in a 65-year-old man with left hemiparesis. CT perfusion maps of cerebral blood volume **(a)**, cerebral blood flow **(b)**, and mean transit time **(c)** show mismatched abnormalities (arrows) that imply the presence of a penumbra. The area with decreased blood volume represents the ischemic core, and that with normal blood volume but decreased blood flow and increased mean transit time is the penumbra.

The perfusion maps can be assessed with a quick visual analysis for color changes that are indicative of perfusion deficits or with a more tedious measurement of perfusion parameters within ROIs placed in multiple regions. Because earlier therapy favors a better outcome of acute stroke, we analyze perfusion maps visually unless we believe that obtaining actual values would be of additional benefit (Fig 11).

Perfused-blood-volume Mapping.—Unenhanced CT followed by CT angiography of the brain can be used to assess both arterial patency and tissue perfusion during the infusion of a single bolus of an iodinated contrast agent. Quantitative cerebral blood volume values are obtained by subtracting the unenhanced CT image data from the CT angiographic source image data (32,34). Since the degree of parenchymal enhancement depends not only on the actual cerebral blood volume but also on the quantity of contrast material that reaches the tissue during the image acquisition, the subtracted images are referred to as perfused-blood-volume maps. Although this technique has an advantage over the first-pass or dynamic CT perfusion imaging technique because of its ability to depict the whole brain, it cannot be used to evaluate cerebral blood flow and mean transit time (and, hence, the penumbra) and is therefore less commonly used.

Results of CT Perfusion Mapping.—The greatest regional abnormalities on CT perfusion maps in acute hemispheric stroke have been demonstrated for mean transit time values, followed by cerebral blood flow and cerebral blood volume values. The mean transit time maps also may be the most sensitive indicators of stroke, with changes in cerebral blood flow and cerebral blood volume being more specific for distinguishing ischemia from infarction (35).

Wintermark et al (36) reported that it was possible to distinguish the penumbra from infarcted tissue in acute stroke patients by defining ischemic tissue (infarct plus penumbra) as cerebral

pixels with a decrease of more than 34% in cerebral blood flow compared with that in clinically normal areas in the cerebral hemispheres. A cerebral blood volume threshold of 2.5 mL/100 g was selected within the ischemic area, and higher and lower values were considered to represent the penumbra and the infarct, respectively. The authors demonstrated significant correlations between *(a)* the penumbra size on initial CT perfusion images and clinical improvement in patients with arterial recanalization (either spontaneous or due to thrombolytic therapy); *(b)* the infarct size at admission CT perfusion imaging and its size at delayed diffusion-weighted MR imaging in patients undergoing recanalization, with the latter likely to be indicative of the recovery of tissue in the penumbra; and *(c)* the size of the combined infarct and penumbra on initial CT perfusion images and the final infarct size on delayed diffusion-weighted MR images in patients without recanalization, a correlation indicative of the expansion of infarction to the penumbra.

In another study by Wintermark et al (37), CT perfusion imaging was more accurate than was unenhanced CT for detecting stroke (75.7%–86.0% vs 66.2%, $P < .01$) and determining the extent of stroke (94.4% vs 42.9%, $P < .01$). Mean transit time maps were more sensitive, while cerebral blood flow and cerebral blood volume maps were more specific for detection of acute stroke. The authors concluded that dynamic CT perfusion mapping was more accurate than unenhanced CT for the detection of hemispheric strokes and that CT perfusion imaging was highly reliable for assessing the extent of the stroke (37).

In a recent study in which the processing and interpretation times of CT angiography and CT perfusion studies were evaluated in patients with acute stroke, the additional acquisition time needed to obtain CT angiograms and CT perfusion maps after the unenhanced CT acquisition was approximately 15 minutes. Furthermore, the combined processing and interpretation times of both CT angiography and CT perfusion studies were less than 10 minutes in three groups of radiologists with varying degrees of expertise (residents, fellows, and consultant neuroradiologists). There was good interobserver agreement also in the identification of intravascular thrombi (κ = 0.95–1.00) and the penumbra (κ = 0.86). The authors concluded that CT angiography and CT perfusion studies in patients with acute stroke could be performed, processed, and interpreted quickly (38).

Thus, unenhanced CT, CT angiography, and CT perfusion imaging can be used in combination for a quick, comprehensive, and accurate evaluation of acute stroke.

Role of MR Imaging in Acute Stroke Evaluation

This section highlights the role of state-of-the-art MR imaging in acute stroke evaluation, with particular emphasis on the importance of diffusion and perfusion MR imaging for evaluating the penumbra. A thorough evaluation of acute stroke can be performed by using a combination of conventional MR imaging, MR angiography, and diffusion- and perfusion-weighted MR imaging techniques.

Conventional MR Imaging

Conventional spin-echo MR imaging is more sensitive and more specific than CT for the detection of acute cerebral ischemia within the first few hours after the onset of stroke. It has the additional benefit of depicting the pathologic entity (stroke and its mimics) in multiple planes. The MR sequences typically used in the evaluation of acute stroke include T1-weighted spin-echo, T2-weighted fast spin-echo, fluid-attenuated inversion recovery, T2*-weighted gradient-echo, and gadolinium-enhanced T1-weighted spin-echo sequences. Typical MR imaging findings in patients with hyperacute cerebral ischemia include hyperintense signal in white matter on T2-weighted images and fluid-attenuated inversion recovery images, with a resultant loss of gray matter–white matter differentiation analogous to the

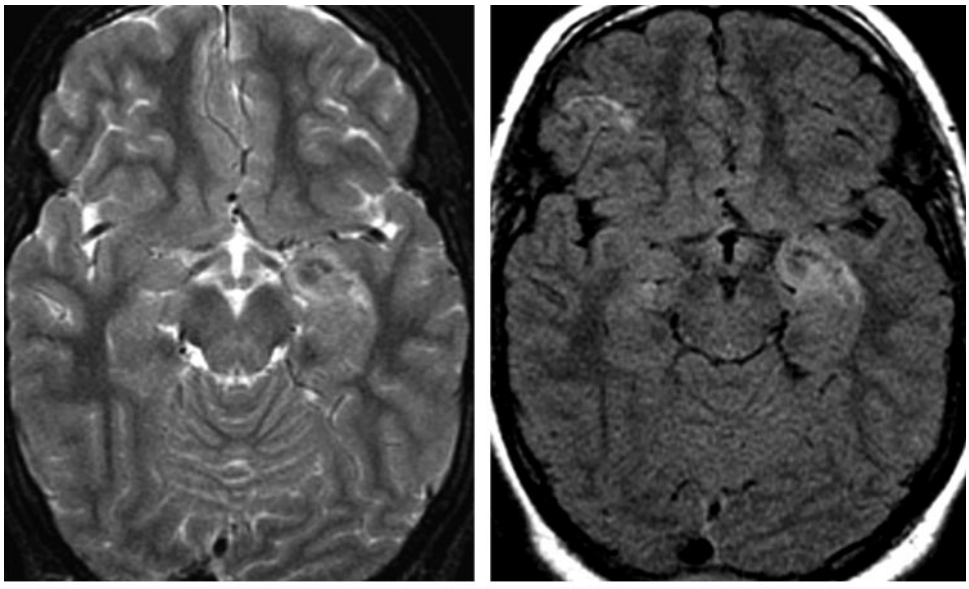

a. b.

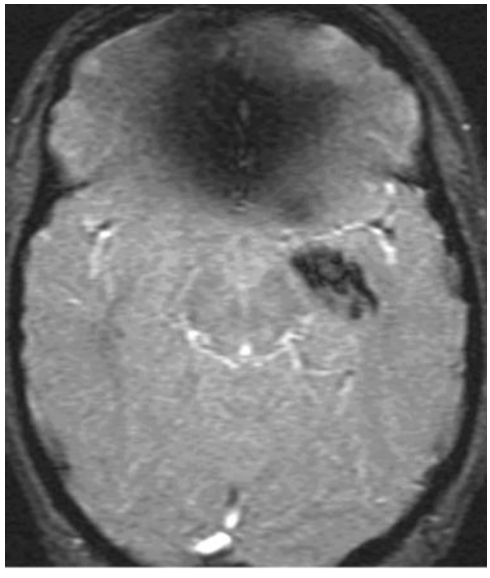

c.

Figure 12. Acute stroke in the left medial temporal lobe in a 44-year-old man. **(a, b)** Axial T2-weighted **(a)** and fluid-attenuated inversion recovery **(b)** images show areas with increased signal intensity. **(c)** Gradient-echo image shows abnormal low signal intensity in the same areas. These findings are suggestive of hemorrhage. (Courtesy of Ellen Hoeffner, MD, University of Michigan Health System, Ann Arbor, Michigan.)

loss at CT (Fig 12); sulcal effacement and mass effect; loss of the arterial flow voids seen on T2-weighted images; and stasis of contrast material within vessels in the affected territories (39,40).

Like the hyperattenuated vessel sign seen at CT, a low-signal-intensity or high-signal-intensity vessel sign due to intravascular thrombus can be seen on MR images obtained with a T2*-weighted gradient-echo or fluid-attenuated inversion recovery sequence, respectively (41,42).

T2*-weighted gradient-echo images depict an acute intracranial hemorrhage as an area of abnormal blooming (Fig 12). Susceptibility-weighted imaging is a recently developed technique that uses both magnitude and phase images from a high-resolution, three-dimensional, fully velocity compensated gradient-echo sequence. Compared with CT and other MR imaging methods, this technique may be a powerful new approach for detecting a cerebral hemorrhage in a patient with acute stroke (43). With the use of techniques such as T2*-weighted MR imaging, very small cerebral hemorrhages are increasingly detectable in patients with acute stroke. However, the risk of thrombolytic therapy in patients with MR imaging–depicted microhemorrhages is unclear, since the present criteria for thrombolysis are based on CT evidence of hemorrhage (44).

Conventional MR imaging is less sensitive than diffusion-weighted MR imaging in the first few hours after a stroke (hyperacute phase) and may result in false-negative findings. Since the advent of diffusion MR imaging, conventional MR imaging sequences play only a relatively minor role in acute stroke imaging, whereas diffusion-weighted sequences may be appropriately included in any MR imaging protocol for evaluation of acute stroke.

MR Angiography

Like CT angiography, MR angiography is useful for detecting intravascular occlusion due to a

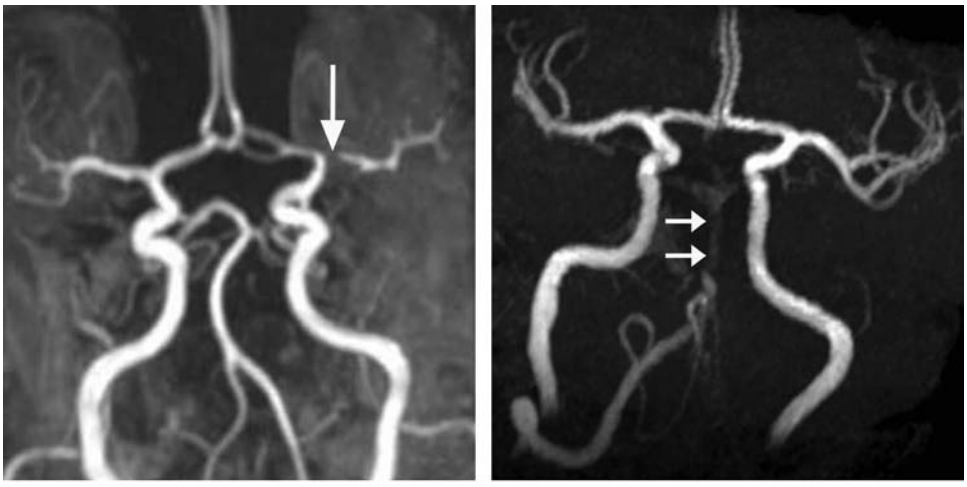

a. b.

Figure 13. Intravascular thrombus. Time-of-flight MR angiograms in two patients with acute stroke symptoms reveal flow gaps in the left proximal middle cerebral artery (arrow in **a**) and the basilar artery (arrows in **b**). Both findings were due to intravascular thrombi, which were confirmed later at digital subtraction angiography. (Courtesy of Ellen Hoeffner, MD, University of Michigan Health System, Ann Arbor, Michigan.)

Figure 14. Acute stroke–induced cytotoxic edema in the right cerebellar hemisphere. Diffusion-weighted MR image (b = 1000 sec/mm^2) shows areas of signal intensity increase due to the restricted mobility of water molecules.

thrombus and for evaluating the carotid bifurcation in patients with acute stroke. Time-of-flight MR angiography and contrast-enhanced MR angiography are commonly used to evaluate the intracranial and extracranial circulation (Fig 13).

Diffusion-weighted MR Imaging

Although diffusion-weighted MR imaging for acute stroke evaluation was introduced in the clinical setting in the mid-1990s, its widespread application was delayed because of the requirement for high-strength magnetic field gradients. Diffusion-weighted imaging sequences now are incorporated into most MR imaging protocols and are essential components of an acute stroke evaluation (45).

Underlying Principles.—The normal motion of water molecules within living tissues is random (brownian motion). In acute stroke, there is an alteration of homeostasis, which normally maintains steady-state proportions of intracellular and extracellular water. Acute stroke causes excess intracellular water accumulation, or cytotoxic edema, with an overall decreased rate of water molecular diffusion within the affected tissue. Measurement of net water molecular motion was first attempted by Stejskal and Tanner (46), who used a T2-weighted spin-echo MR imaging sequence with two extra gradient pulses that were equal in magnitude and opposite in direction. For various reasons, this technique results in a loss of signal in tissue. Tissues with a higher rate of diffusion undergo a greater loss of signal in a given period of time than do tissues with a lower diffusion rate. Therefore, areas of cytotoxic edema, in which the motion of water molecules is restricted, appear brighter on diffusion-weighted images because of lesser signal losses (Figs 14, 15). On diffusion-weighted images from patients with hyperacute stroke, ischemic tissue appears bright in comparison with normal brain tissue (39,45,46).

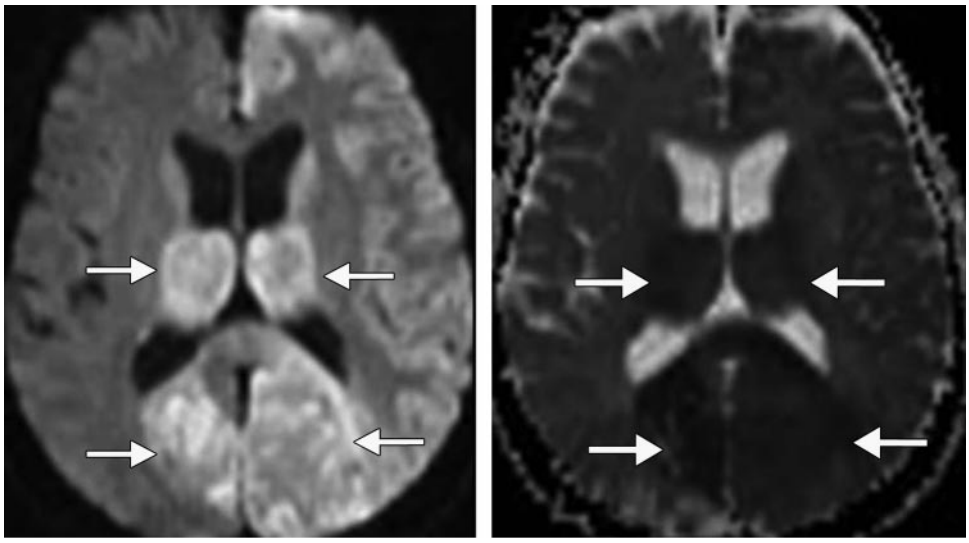

a. b.

Figure 15. Acute stroke of the posterior circulation in a 77-year-old man. **(a)** Diffusion-weighted MR image (b = 1000 sec/mm^2) shows bilateral areas of increased signal intensity (arrows) in the thalami and occipital lobes. **(b)** ADC map shows decreased ADC values in the same areas (arrows). These findings are indicative of acute ischemia.

Current diffusion-weighted MR imaging techniques employ echo-planar sequences that are highly resistant to patient motion. Image acquisition can be performed in a few seconds to 2 minutes and has increased sensitivity to signal changes that are due to molecular motion (45). Other methods of diffusion imaging include single-shot gradient-echo, single-shot spin-echo, and single-shot fast spin-echo techniques; line scan diffusion-weighted imaging; and spiral diffusion-weighted MR imaging (47–50).

The actual diffusion coefficient cannot be measured by using diffusion-weighted MR imaging, for a number of reasons (including the inability of diffusion-weighted imaging to depict the difference between molecular motion due to concentration gradients and molecular motion due to thermal or pressure gradients or ionic interactions) (45). Hence, the diffusion coefficient obtained from orthogonal diffusion-weighted MR images in all three planes is called the apparent diffusion coefficient (ADC). The importance of interpreting diffusion-weighted MR images by comparing them with ADC maps is explored in a later section.

Clinical Application.—Restricted diffusion has been observed in animals as early as 10 minutes after the onset of ischemia, with a pseudonormalization of ADC values occurring at approximately 2 days. However, the time course of diffusion changes in humans is more prolonged. In humans, diffusion restriction with reduced ADC has been observed as early as 30 minutes after the onset of ischemia. The ADC continues to decrease further and reaches a nadir at approximately 3–5 days. Thereafter, the ADC starts to increase again, and it returns to the baseline value at approximately 1–4 weeks. This is likely due to the development of vasogenic edema along with the persistence of cytotoxic edema. In a few weeks to months, gliosis develops, with a resultant increase in the quantity of extracellular water (45,51).

This same pattern of change can be observed in the diffusion-weighted MR imaging appearance of ischemic human brain tissue during the evolution of acute stroke: Hyperintense signal is seen with reduced ADC values from approximately 30 minutes to 5 days after the onset of symptoms (Figs 14, 15); mildly hyperintense signal is seen with pseudonormal ADC values at 1–4 weeks; and variable signal intensity (because of T2 characteristics) is seen with increased ADC values several weeks to months after symptom onset (Fig 16).

The signal intensity in areas affected by acute stroke on diffusion-weighted images, thus, increases during the 1st week after symptom onset and decreases thereafter; however, the signal may remain hyperintense for a longer period (52). Increased intensity of the diffusion-weighted imaging signal in the initial few days is due to restricted diffusion and thereafter is due to an increase of the T2 signal (T2 shine-through) from the infarcted tissue.

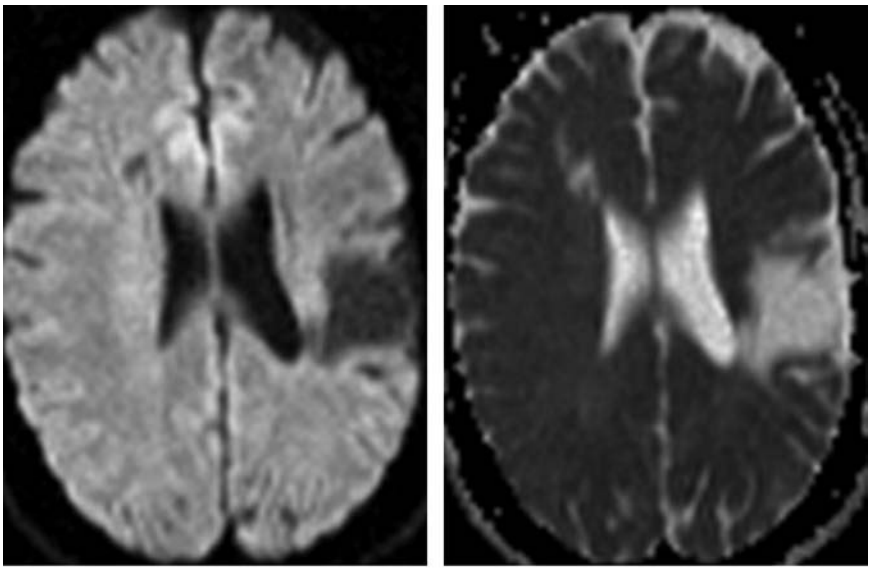

a. b.

Figure 16. Chronic infarcts in a 71-year-old man with a remote history of multiple strokes. **(a)** Diffusion-weighted MR image (b = 1000 sec/mm^2) shows areas of decreased signal intensity in the left frontal lobe. **(b)** ADC map shows increased ADC values in the white matter of the right frontal lobe. These features are suggestive of chronic infarction.

Teaching Point

Hence, the diffusion-weighted imaging signal cannot be used alone to reliably estimate infarct age; it is important to examine diffusion-weighted images in comparison with ADC maps.

Tissues in which ADC values are reduced almost always undergo irreversible infarction; the decrease in ADC values is only rarely reversible with thrombolytic therapy (53). However, earlier pseudonormalization of ADC values in 1–2 days has been observed in patients who received intravenous thrombolytic drug therapy within 3 hours after stroke onset (54).

In contrast to unenhanced CT or conventional MR imaging, which have low sensitivities (<50%) for acute ischemia detection within the first 6 hours after onset, diffusion-weighted imaging was reported to have had high sensitivity and specificity, of 88%–100% and 86%–100%, respectively, in various studies (53,55,56). In patients with very small lacunar brainstem infarction or deep gray nuclei infarction, diffusion-weighted imaging findings may be false-negative (55,56). Ischemic regions that are still viable initially may appear normal on diffusion-weighted images (referred to as false-negative diffusion-weighted images by some authors) even in the presence of decreased perfusion (increased mean transit time and decreased cerebral blood flow). In patients with ischemia that later progresses to infarction, diffusion-weighted images show restricted diffusion in these regions (45). Thus, the early finding of normal diffusion-weighted images and altered perfusion parameters suggests the presence of tissue that is at risk. Such a finding should lead to the initiation of therapy to prevent infarction, if that therapy is clinically feasible and appropriate. Findings of acute ischemia at diffusion-weighted imaging may be false-positive in the presence of a cerebral abscess (in which diffusion is restricted primarily by viscosity) or tumor (a lesion with a high nuclear-cytoplasmic ratio, such as lymphoma), but such lesions usually can be differentiated from acute ischemia on the basis of their appearance on conventional MR images (45).

Correlation of Imaging Features with Clinical Outcomes.—Statistically significant correlations have been demonstrated repeatedly between the acute infarct volume on diffusion-weighted images and various neurologic scales for the assessment of acute and chronic stroke, including the NIHSS, Canadian Neurologic Scale, Barthel Index, and Rankin Scale (45,51,57,58). It also has been shown that patients who have lesions with a larger volume on perfusion-weighted MR images than on diffusion-weighted MR images have worse outcomes and larger final infarct volumes (59). Thus, the evaluation of images for a diffusion-perfusion mismatch at a very early stage of stroke may help predict the clinical outcome.

Perfusion-weighted MR Imaging

While diffusion-weighted MR imaging is most useful for detecting irreversibly infarcted tissue, perfusion-weighted imaging may be used to identify areas of reversible ischemia as well. Perfusion-weighted MR imaging techniques rely either on an exogenous method of achieving perfusion contrast (ie, the administration of an MR contrast agent) or on an endogenous method (ie, the labeling of hydrogen-1 protons in water, also known as arterial spin labeling). Exogenous techniques are

typically susceptibility based and depend on T2* effects, but they may be T1 weighted instead. Dynamic susceptibility-weighted (T2*-weighted) sequences probably are most commonly used in acute stroke evaluation, while the other MR perfusion imaging techniques are more commonly used in tumor evaluation or other applications (45).

Underlying Principles.—The passage of an intravascular MR contrast agent through the brain capillaries causes a transient loss of signal because of the T2* effects of the contrast agent. The dynamic contrast-enhanced MR perfusion imaging technique involves tracking of the tissue signal changes caused by susceptibility (T2*) effects to create a hemodynamic time–signal intensity curve (Fig 17). As in dynamic CT perfusion imaging, perfusion maps of cerebral blood volume and mean transit time can be calculated from this curve by using a deconvolution technique (60–62).

In contrast, the arterial spin labeling technique does not require the use of an exogenous contrast agent; instead, it exploits the spins of endogenous water protons to measure perfusion. The spin polarity of arterial protons flowing into the imaging plane is inverted by applying radiofrequency pulses upstream from the imaging section. The effect on image intensity is measured as these protons perfuse the brain tissue. Two sets of images are obtained, one that is flow sensitive and one that is insensitive to flow. The image obtained by subtracting the flow-sensitive image from the flow-insensitive image provides a measure of the labeled protons that perfused the imaging plane. Perfusion parameters then can be calculated from the subtracted image (63,64).

Clinical Application.—Among the various types of perfusion maps, maps of the mean transit time generally show the largest area of abnormality and often reflect an overestimation of the final infarct size, whereas maps of cerebral blood volume tend toward underestimation of the final infarct size. It also has been noted that a mismatch between initial cerebral blood flow maps and diffusion-weighted images more often predicted a further extension of the infarct than did a mismatch between cerebral blood volume maps and diffusion-weighted images. Cerebral blood volume maps were most closely correlated with changes in infarct size between initial and follow-up diffusion-weighted MR imaging (61).

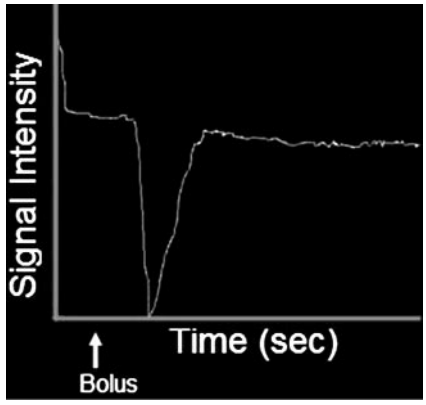

Figure 17. Time–signal intensity curve illustrates the decrease in signal intensity within an ROI after the administration of an MR contrast agent bolus. The signal intensity decrease is due to the T2* effect of the contrast agent, an effect that is exploited in dynamic susceptibility-weighted MR perfusion imaging to calculate perfusion parameters.

Comparison of Diffusion and Perfusion Abnormalities

When the appearance of a lesion on diffusion-weighted MR images is compared with that on perfusion-weighted MR images obtained with acute stroke imaging protocols, one of the following three patterns is observed (51,59,61,65):

1. The lesion appears smaller on the diffusion-weighted images than on the perfusion-weighted images. This is typically observed in large-vessel strokes (Fig 18). In the acute stroke setting, a region that shows both diffusion and perfusion abnormalities is thought to represent irreversibly infarcted tissue, while a region that shows only perfusion abnormalities and has normal diffusion likely represents viable ischemic tissue, or a penumbra. Normal diffusion with altered perfusion parameters (increased mean transit time with normal cerebral blood volume and normal cerebral blood flow) also can be seen during challenge testing in patients with symptomatic chronic cerebrovascular disease and inadequate collateral circulation or with chronic cerebrovascular disease and adequate collateral circulation.

Teaching Point

2. The lesion has the same size on diffusion-weighted images and perfusion-weighted images. This occurs when the tissue is irreversibly infarcted and there is no penumbra.

3. The lesion appears larger on diffusion-weighted images than on perfusion-weighted images or is seen only on diffusion-weighted images and not perfusion-weighted images. These findings are usually associated with early reperfusion of ischemic tissue, and the size of the lesion on

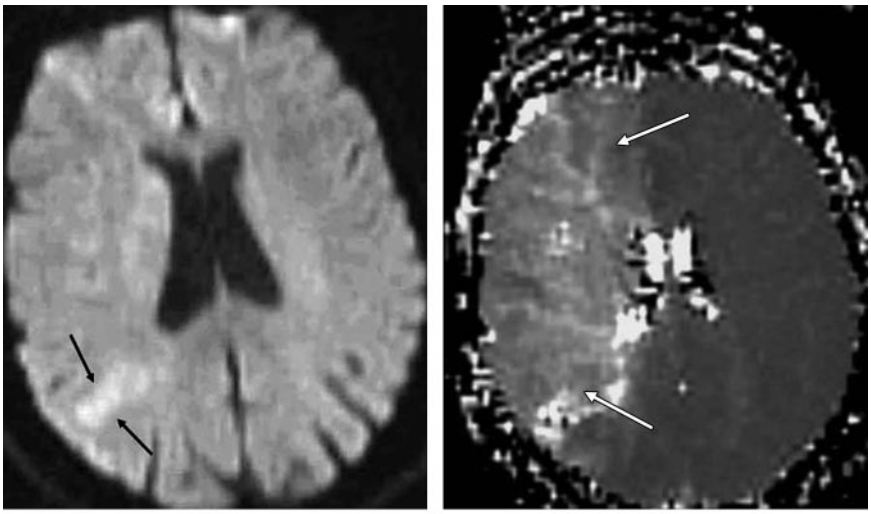

a. b.

Figure 18. Acute stroke in a 67-year-old woman with acute left hemiplegia 2 hours after carotid endarterectomy. **(a)** Diffusion-weighted MR image (b = 1000 sec/mm^2) shows an area of mildly increased signal intensity in the right parietal lobe (arrows). The ADC values in this region were decreased. **(b)** Perfusion-weighted MR image shows a larger area with increased time to peak enhancement (arrows) in the right cerebral hemisphere. The mismatch between the perfusion and diffusion images is indicative of a large penumbra.

Table 5
Technique Selection for the Evaluation of Acute Stroke with CT and MR Imaging

Area to Be Evaluated	CT	MR Imaging
Parenchyma	Unenhanced CT	Conventional MR imaging and diffusion-weighted imaging
Blood vessels (pipes)	CT angiography	MR angiography
Perfusion	CT perfusion imaging	Perfusion-weighted imaging
Penumbra	Mismatch between cerebral blood flow and blood volume	Mismatch between diffusion-weighted and perfusion-weighted imaging findings

Table 6
Comparison of CT and MR Imaging for Evaluation of Acute Stroke

Characteristic	CT	MR Imaging
Availability	Good	Fair
Examination time (min)	5	15
Imaging volume for perfusion study	2–4 cm	Entire brain
Risks to patient		
Radiation	Ionizing radiation associated with potential risks for cancer	No ionizing radiation
Contrast material	Iodinated contrast medium is mandatory, and patients incur higher risks for anaphylaxis and toxic effects on the kidneys	Gadolinium-based contrast medium is mandatory, with a minimally increased risk for toxic effects on the kidneys

diffusion-weighted images does not usually change substantially over time.

CT versus MR Imaging in Acute Stroke Evaluation

The specific uses of various CT and MR imaging techniques in acute stroke evaluation are summarized in Table 5, and the relative advantages and disadvantages of the two modalities are detailed in Table 6. CT is widely available, and a stroke imaging protocol that consists of unenhanced CT, CT angiography, and CT perfusion imaging can be executed in 5 minutes for the comprehensive evaluation of the extra- and intracranial circulation, the amount of infarcted brain tissue, and the penumbra (66). The MR imaging protocol for evaluation of stroke, which includes conventional MR imaging, diffusion-weighted imaging, MR

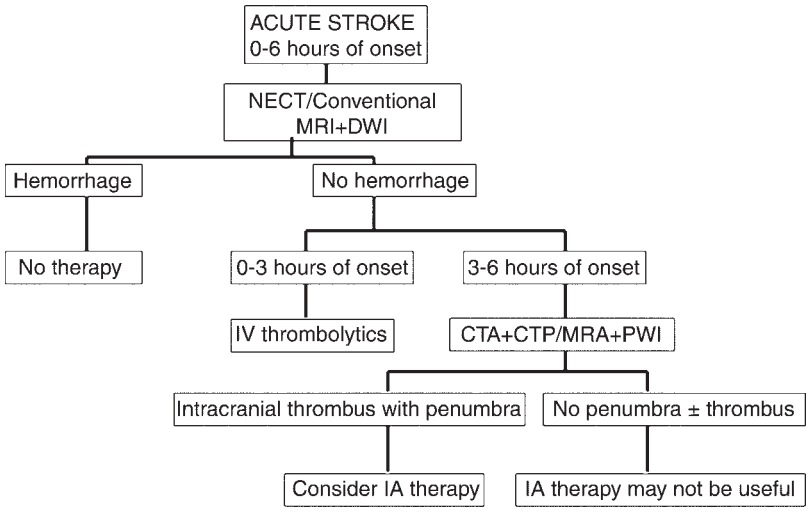

Figure 19. Flow chart shows an acute stroke imaging protocol. *CTA* = CT angiography, *CTP* = CT perfusion imaging, *DWI* = diffusion-weighted MR imaging, *IA* = intraarterial, *IV* = intravenous, *MRA* = MR angiography, *MRI* = conventional MR imaging, *NECT* = unenhanced CT, *PWI* = perfusion-weighted MR imaging.

angiography, and perfusion-weighted imaging, may take a little longer (15 minutes) (66). The two modalities are equally useful for evaluating acute stroke and provide equivalent depiction of the penumbra. Good correlations have been demonstrated between perfusion parameters on CT perfusion maps and those on perfusion-weighted MR images and between the extent of the infarct on CT perfusion maps and that on diffusion-weighted MR images (32,67,68). Some authors have pointed out that whereas CT is simple to perform, MR findings are simple to interpret (eg, diffusion-weighted images are easier to interpret with minimal requisite training than are CT angiographic images and CT perfusion maps). While the debate about which modality is best will likely continue into the near future, it is important to remember that both modalities currently have a role in acute stroke evaluation, depending on the clinical circumstances and on local constraints such as the availability of technology and the experience of the staff (66).

Acute Stroke Imaging Protocol

Acute stroke imaging protocols vary among institutions, depending on the availability of imaging time, software, and expertise. We use a simple protocol that we believe is applicable at most institutions (Fig 19). In this protocol, when acute stroke patients present within 6 hours of the onset of symptoms, they are examined either with unenhanced CT or with conventional and diffusion-weighted MR imaging. Whereas the demonstration of hemorrhage at unenhanced CT is a contraindication to thrombolytic therapy, it is unclear whether the depiction of microhemorrhages on gradient-echo MR images is an absolute contraindication to thrombolytic therapy. The decision to treat depends on the clinical status of the patient and the estimated risk-to-benefit ratio of therapy. Patients in whom more than one-third of the MCA territory is involved in acute ischemia are not treated with thrombolytic drugs. Among patients with ischemia of less than one-third of the MCA territory, those who present within 3 hours after the onset of acute stroke are given intravenous thrombolytic drugs and appropriate supportive therapy after informed consent is obtained. Patients who present within 3–6 hours after the onset of symptoms are further examined with CT angiography and CT perfusion imaging or with MR angiography and perfusion-weighted MR imaging to assess the status of the intracranial and neck vessels and detect any penumbra. Intraarterial therapy is usually considered for patients in whom a penumbra is seen, and the aggressiveness of therapy (intraarterial administration of thrombolytic drugs vs more aggressive mechanical thrombolysis) is tailored to each patient. Patients in whom no penumbra is seen are not usually treated with thrombolytic drugs, since the risk-to-benefit ratio of such therapy may be unfavorable.

The Future

In future, the selection of patients for thrombolytic therapy may be made more effective by performing appropriate imaging studies rather than relying on the time of onset as the sole determinant of selection. In a recent trial (3), intravenous desmoteplase administration at 3–9 hours after the onset of acute ischemia was associated with a higher rate of reperfusion and a better clinical outcome than placebo in patients selected because of a mismatch between findings on diffusion and perfusion MR images. The symptomatic intracranial hemorrhage rate with desmoteplase

was low with the use of a dose of 125 μg/kg or less (3). That result was supported by findings in another recent desmoteplase dose-escalation study, in which doses of 90 μg/kg and 125 μg/kg were investigated in patients with a diffusion-perfusion mismatch at MR imaging performed 3–9 hours after the onset of acute ischemic stroke (7). The authors found that a dose of 125 μg/kg desmoteplase appeared to improve the clinical outcome, especially that in patients who fulfilled all the MR imaging criteria, and there were no symptomatic intracranial hemorrhages in the study population (7).

Another emerging technique that may be of benefit in acute stroke evaluation is MR permeability imaging, which is based on dynamic contrast-enhanced imaging and subsequent kinetic modeling of microvascular permeability and which allows quantitation of defects in the blood-brain barrier (69). The identification of patients with a loss of integrity of the blood-brain barrier, who are thought to have an increased risk of hemorrhagic transformation with thrombolytic therapy, may help reduce morbidity and mortality (69). In a recent investigation of the role of MR permeability imaging in acute stroke, three of the 10 patients in whom defects were identified in the blood-brain barrier did undergo a hemorrhagic transformation. This result may support the hypothesis that blood-brain barrier integrity is closely related to the risk of hemorrhagic transformation. The authors concluded that the addition of MR permeability imaging to the acute stroke evaluation protocol may aid in the selection of patients for thrombolytic drug therapy and may help decrease morbidity and mortality. They also concluded that therapy with intravenous thrombolytic drugs is feasible more than 3 hours after symptom onset in patients with an intact blood-brain barrier (69).

As technologic advances result in faster and more accurate image acquisition, the emphasis in acute stroke evaluation is likely to shift from simple anatomic imaging to functional imaging to determine the viability of tissue and the appropriateness of therapy. Variations in the threshold for identification of a penumbra at imaging, which depend on the technique used, may cause inaccuracies in detection and quantification of the penumbra and may make comparisons difficult between imaging studies obtained with different techniques. A penumbra identification based on the cascade of molecular events that are responsible for the evolution of the penumbra toward infarction may be more reliable. Hence, molecular imaging may aid in the accurate and early detection of the penumbra. Future research in this direction may lead to a better understanding and improved targeting of cytoprotective and cytotoxic mechanisms for effective neuroprotection (70).

Conclusion

Imaging technology has advanced rapidly in the past 2 decades, and current imaging techniques can be used to identify hyperacute stroke and guide therapy by providing information about the functional status of ischemic brain tissue. Both CT and MR imaging are useful for the comprehensive evaluation of acute stroke and can provide important and necessary information for therapy planning.

Acknowledgments: We thank Suzanne Murphy, Sarah Abate, and Anne Phillips for help with the illustrations.

References

1. Beauchamp NJ Jr, Barker PB, Wang PY, vanZijl PC. Imaging of acute cerebral ischemia. Radiology 1999;212:307–324.
2. Tissue plasminogen activator for acute ischemic stroke. The National Institute of Neurological Disorders and Stroke rt-PA Stroke Study Group. N Engl J Med 1995;333:1581–1587.
3. Hacke W. The Desmoteplase in Acute Ischemic Stroke Trial (DIAS): a phase II MRI-based 9-hour window acute stroke thrombolysis trial with intravenous desmoteplase. Stroke 2005;36:66–73.
4. Rowley HA. The four Ps of acute stroke imaging: parenchyma, pipes, perfusion, and penumbra. AJNR Am J Neuroradiol 2001;22:599–601.
5. Astrup J, Siesjo BK, Symon L. Thresholds in cerebral ischemia: the ischemic penumbra. Stroke 1981;12:723–725.
6. Hössmann KA. Viability thresholds and the penumbra of focal ischemia. Ann Neurol 1994;36: 557–565.
7. Furlan AJ, Eyding D, Albers GW, et al; and the DEDAS Investigators. Dose Escalation of Desmoteplase for Acute Ischemic Stroke (DEDAS): evidence of safety and efficacy 3 to 9 hours after stroke onset. Stroke 2006;37:1227–1231.
8. Tomandl BF, Klotz E, Handschu R, et al. Comprehensive imaging of ischemic stroke with multisection CT. RadioGraphics 2003;23:565–592.
9. Leys D, Pruvo JP, Godefroy O, Rondepierre P, Leclerc X. Prevalence and significance of hyperdense middle cerebral artery in acute stroke. Stroke 1992;23:317–324.
10. Bastianello S, Pierallini A, Colonnese C, et al. Hyperdense middle cerebral artery CT sign: comparison with angiography in the acute phase of ischemic supratentorial infarction. Neuroradiology 1991;33:207–211.
11. von Kummer R, Meyding-Lamade U, Forsting M, et al. Sensitivity and prognostic value of early CT in occlusion of the middle cerebral artery trunk. AJNR Am J Neuroradiol 1994;15:9–15.
12. Tomsick TA, Brott TG, Olinger CP, et al. Hyperdense middle cerebral artery: incidence and

quantitative significance. Neuroradiology 1989; 31:312–315.
13. von Kummer R, Holle R, Gizyska U, et al. Interobserver agreement in assessing early CT signs of middle cerebral artery infarction. AJNR Am J Neuroradiol 1996;17:1743–1748.
14. Lee TC, Bartlett ES, Fox AJ, Symons SP. The hypodense artery sign. AJNR Am J Neuroradiol 2005;26:2027–2029.
15. Tomura N, Uemura K, Inugami A, Fujita H, Higano S, Shishido F. Early CT finding in cerebral infarction: obscuration of the lentiform nucleus. Radiology 1988;168:463–467.
16. Truwit CL, Barkowich AJ, Gean-Marton A, Hibri N, Norman D. Loss of the insular ribbon: another early CT sign of acute middle cerebral artery infarction. Radiology 1990;176:801–806.
17. Lev MH, Farkas J, Gemmete JJ, et al. Acute stroke: improved nonenhanced CT detection—benefits of soft-copy interpretation by using variable window width and center level settings. Radiology 1999;213:150–155.
18. Hacke W, Kaste M, Fieschi C, et al. Intravenous thrombolysis with recombinant tissue plasminogen activator for acute hemispheric stroke. The European Cooperative Acute Stroke Study (ECASS). JAMA 1995;274:1017–1025.
19. Dippel DW, Du Ry van Beest Holle M, van Kooten F, Koudstaal PJ. The validity and reliability of signs of early infarction on CT in acute ischaemic stroke. Neuroradiology 2000;42:629–633.
20. Schriger DL, Kalafut M, Starkman S, Krueger M, Saver JL. Cranial computed tomography interpretation in acute stroke: physician accuracy in determining eligibility for thrombolytic therapy. JAMA 1998;279:1293–1297.
21. Grotta JC, Chiu D, Lu M, et al. Agreement and variability in the interpretation of early CT changes in stroke patients qualifying for intravenous rtPA. Stroke 1999;30:1528–1533.
22. Wardlaw JM, Dorman PJ, Lewis SC, Sandercock PA. Can stroke physicians and neurologists identify signs of early cerebral infarction on CT? J Neurol Neurosurg Psychiatry 1999;67:651–653.
23. Pexman JH, Barber PA, Hill MD, et al. Use of the Alberta Stroke Program Early CT Score (ASPECTS) for assessing CT scans in patients with acute stroke. AJNR Am J Neuroradiol 2001;22: 1534–1542.
24. Katz DA, Marks MP, Napel SA, Bracci PM, Roberts SL. Circle of Willis: evaluation with spiral CT angiography, MR angiography, and conventional angiography. Radiology 1995;195:445–449.
25. Barnwell SL, Clark WM, Nguyen TT, O'Neill OR, Wynn ML, Coull BM. Safety and efficacy of delayed intraarterial urokinase therapy with mechanical clot disruption for thromboembolic stroke. AJNR Am J Neuroradiol 1994;15:1817–1822.
26. Zeumer H, Freitag HJ, Zanella F, Thie A, Arning C. Local intra-arterial fibrinolytic therapy in patients with stroke: urokinase versus recombinant tissue plasminogen activator (r-tPA). Neuroradiology 1993;35:159–162.
27. Sims JR, Rordorf G, Smith EE, et al. Arterial occlusion revealed by CT angiography predicts NIH stroke score and acute outcomes after IV tPA treatment. AJNR Am J Neuroradiol 2005;26:246–251.
28. Koenig M, Klotz E, Luka B, Venderink DJ, Spittler JF, Heuser L. Perfusion CT of the brain: diagnostic approach for early detection of ischemic stroke. Radiology 1998;209:85–93.
29. Nabavi DG, Cenic A, Craen RA, et al. CT assessment of cerebral perfusion: experimental validation and initial clinical experience. Radiology 1999;213:141–149.
30. Wintermark M, Maeder P, Thiran JP, Schnyder P, Meuli R. Quantitative assessment of regional cerebral blood flow by perfusion CT studies at low injection rates: a critical review of the underlying theoretical models. Eur Radiol 2001;11:1220–1230.
31. Hoeffner EG, Case I, Jain R, et al. Cerebral perfusion CT: technique and clinical applications. Radiology 2004;231:632–644.
32. Eastwood JD, Lev MH, Provenzale JM. Perfusion CT with iodinated contrast material. AJR Am J Roentgenol 2003;180:3–12.
33. Wirestam R, Andersson L, Ostergaard L, et al. Assessment of regional cerebral blood flow by dynamic susceptibility contrast MRI using different deconvolution techniques. Magn Reson Med 2000;43:691–700.
34. Alpert NM, Berdichevsky D, Levin Z, Thangaraj V, Gonzalez G, Lev MH. Performance evaluation of an automated system for registration and postprocessing of CT scans. J Comput Assist Tomogr 2001;25:747–752.
35. Eastwood JD, Lev MH, Azhari T, et al. CT perfusion scanning with deconvolution analysis: pilot study in patients with acute middle cerebral artery stroke. Radiology 2002;222:227–236.
36. Wintermark M, Reichhart M, Thiran JP, et al. Prognostic accuracy of cerebral blood flow measurement by perfusion computed tomography, at the time of emergency room admission, in acute stroke patients. Ann Neurol 2002;51:417–432.
37. Wintermark M, Fischbein NJ, Smith WS, Ko NU, Quist M, Dillon WP. Accuracy of dynamic perfusion CT with deconvolution in detecting acute hemispheric stroke. AJNR Am J Neuroradiol 2005;26:104–112.
38. Srinivasan A, Goyal M, Lum C, Nguyen T, Miller W. Processing and interpretation times of CT angiogram and CT perfusion studies in stroke. Can J Neurol Sci 2005;32:483–486.
39. Provenzale JM, Jahan R, Naidich TP, Fox AJ. Assessment of the patient with hyperacute stroke: imaging and therapy. Radiology 2003;229:347–359.
40. Elster AD, Moody DM. Early cerebral infarction: gadopentetate dimeglumine enhancement. Radiology 1990;177:627–632.
41. Schellinger PD, Chalela JA, Kang DW, Latour LL, Warach S. Diagnostic and prognostic value of early MR imaging vessel signs in hyperacute stroke patients imaged <3 hours and treated with recombinant tissue plasminogen activator. AJNR Am J Neuroradiol 2005;26:618–624.

42. Rovira A, Orellana P, Alvarez-Sabin J, et al. Hyperacute ischemic stroke: middle cerebral artery susceptibility sign at echo-planar gradient-echo MR imaging. Radiology 2004;232:466–473.
43. Wycliffe ND, Choe J, Holshouser B, Oyoyo UE, Haacke EM, Kido DK. Reliability in detection of hemorrhage in acute stroke by a new three-dimensional gradient recalled echo susceptibility-weighted imaging technique compared to computed tomography: a retrospective study. J Magn Reson Imaging 2004;20:372–377.
44. Viswanathan A, Chabriat H. Cerebral microhemorrhage. Stroke 2006;37:550–555.
45. Schaefer PW, Grant PE, Gonzalez RG. Diffusion-weighted MR imaging of the brain. Radiology 2000;217:331–345.
46. Stejskal E, Tanner J. Spin diffusion measurements: spin echoes in the presence of a time-dependent field gradient. J Chem Phys 1965; 42:288–292.
47. Liu G, van Gelderen P, Duyn J, Moonen CT. Single-shot diffusion MRI of human brain on a conventional clinical instrument. Magn Reson Med 1996;35:671–677.
48. Beaulieu CF, Zhou X, Cofer GP, Johnson GA. Diffusion-weighted MR microscopy with fast spin-echo. Magn Reson Med 1993;30:201–206.
49. Gudbjartsson H, Maier SE, Mulkern RV, Morocz IA, Patz S, Jolesz FA. Line scan diffusion imaging. Magn Reson Med 1996;36:509–519.
50. de Crespigny AJ, Marks MP, Enzmann DR, Moseley ME. Navigated diffusion imaging of normal and ischemic human brain. Magn Reson Med 1995;33:720–728.
51. Schwamm LH, Koroshetz WJ, Sorensen AG, et al. Time course of lesion development in patients with acute stroke: serial diffusion- and hemodynamic-weighted magnetic resonance imaging. Stroke 1998;29:2268–2276.
52. Lansberg MG, Thijs VN, O'Brien MW, et al. Evolution of apparent diffusion coefficient, diffusion-weighted, and T2-weighted signal intensity of acute stroke. AJNR Am J Neuroradiol 2001;22: 637–644.
53. Marks MP, de Crespigny A, Lentz D, Enzmann DR, Albers GW, Moseley ME. Acute and chronic stroke: navigated spin-echo diffusion-weighted MR imaging. Radiology 1996;199:403–408.
54. Marks MP, Tong DC, Beaulieu C, Albers GW, de Crespigny A, Moseley ME. Evaluation of early reperfusion and i.v. tPA therapy using diffusion- and perfusion-weighted MRI. Neurology 1999;52: 1792–1798.
55. Gonzalez RG, Schaefer PW, Buonanno FS, et al. Diffusion-weighted MR imaging: diagnostic accuracy in patients imaged within 6 hours of stroke symptom onset. Radiology 1999;210:155–162.
56. Lovblad KO, Laubach HJ, Baird AE, et al. Clinical experience with diffusion-weighted MR in patients with acute stroke. AJNR Am J Neuroradiol 1998;19:1061–1066.
57. Lovblad KO, Baird AE, Schlaug G, et al. Ischemic lesion volumes in acute stroke by diffusion-weighted magnetic resonance imaging correlate with clinical outcome. Ann Neurol 1997;42: 164–170.
58. Tong DC, Yenari MA, Albers GW, O'Brien M, Marks MP, Moseley ME. Correlation of perfusion- and diffusion-weighted MRI with NIHSS score in acute (<6.5 hour) ischemic stroke. Neurology 1998;50:864–870.
59. Barber PA, Darby DG, Desmond PM, et al. Prediction of stroke outcome with echoplanar perfusion- and diffusion-weighted MRI. Neurology 1998;51:418–456.
60. Edelman RR, Mattle HP, Atkinson DJ, et al. Cerebral blood flow: assessment with dynamic contrast-enhanced T2*-weighted MR imaging at 1.5 T. Radiology 1990;176:211–220.
61. Sorensen AG, Buonanno FS, Gonzalez RG, et al. Hyperacute stroke: evaluation with combined multisection diffusion-weighted and hemodynamically weighted echo-planar MR imaging. Radiology 1996;199:391–401.
62. Ostergaard L. Principles of cerebral perfusion imaging by bolus tracking. J Magn Reson Imaging 2005;22:710–717.
63. Thomas DL. Arterial spin labeling in small animals: methods and applications to experimental cerebral ischemia. J Magn Reson Imaging 2005; 22:741–744.
64. Chalela JA, Alsop DC, Gonzalez-Atavales JB, Maldjian JA, Kasner SE, Detre JA. Magnetic resonance perfusion imaging in acute ischemic stroke using continuous arterial spin labeling. Stroke 2000;31:680–687.
65. Eskey CJ, Sanelli PC. Perfusion imaging of cerebrovascular reserve. Neuroimaging Clin N Am 2005;15:367–381.
66. Zimmerman RD. Stroke wars: episode IV—CT strikes back. AJNR Am J Neuroradiol 2004;25: 1304–1309.
67. Schramm P, Schellinger PD, Klotz E, et al. Comparison of perfusion computed tomography and computed tomography angiography source images with perfusion-weighted imaging and diffusion-weighted imaging in patients with acute stroke of less than 6 hours' duration. Stroke 2004;35:1652–1658.
68. Galvez M, York GE 2nd, Eastwood JD. CT perfusion parameter values in regions of diffusion abnormalities. AJNR Am J Neuroradiol 2004;25: 1205–1210.
69. Kassner A, Roberts T, Taylor K, Silver F, Mikulis D. Prediction of hemorrhage in acute ischemic stroke using permeability MR imaging. AJNR Am J Neuroradiol 2005;26:2213–2217.
70. Castellanos M, Sobrino T, Castillo J. Evolving paradigms for neuroprotection: molecular identification of ischemic penumbra. Cerebrovasc Dis 2006;21(suppl 2):71–79.

This article meets the criteria for 1.0 credit hour in category 1 of the AMA Physician's Recognition Award. To obtain credit, see accompanying test at http://www.rsna.org/education/rg_cme.html.

State-of-the-Art Imaging of Acute Stroke

Ashok Srinivasan, MD, et al

RadioGraphics 2006; 26:S75–S95 • **Published online** 10.1148/rg.26si065501 • **Content Codes:** CT MR NR

Page S76
Acute cerebral ischemia may result in a central irreversibly infarcted tissue core surrounded by a peripheral region of stunned cells that is called a penumbra. Evoked potentials in the peripheral region are abnormal, and the cells have ceased to function, but this region is potentially salvageable with early recanalization.

Page S78
Detection of early acute ischemic stroke on unenhanced CT images may be improved by using variable window width and center level settings to accentuate the contrast between normal and edematous tissue.

Page S82
The clinical application of CT perfusion imaging in acute stroke is based on the hypothesis that the penumbra shows either *(a)* increased mean transit time with moderately decreased cerebral blood flow (>60%) and normal or increased cerebral blood volume (80%–100% or higher) secondary to autoregulatory mechanisms or *(b)* increased mean transit time with markedly reduced cerebral blood flow (>30%) and moderately reduced cerebral blood volume (>60%), whereas infarcted tissue shows severely decreased cerebral blood flow (<30%) and cerebral blood volume (<40%) with increased mean transit time.

Page 89
The diffusion-weighted imaging signal cannot be used alone to reliably estimate infarct age; it is important to examine diffusion-weighted images in comparison with ADC maps.

Pages S90
In the acute stroke setting, a region that shows both diffusion and perfusion abnormalities is thought to represent irreversibly infarcted tissue, while a region that shows only perfusion abnormalities and has normal diffusion likely represents viable ischemic tissue, or a penumbra.